Am J Transl Res 2024;16(6):2263-2277
www.ajtr.org /ISSN:1943-8141/AJTR0157361

Original Article

Role of vascular endothelial growth factor D in lung adenocarcinoma immunotherapy response

Xiaoling Du[1,2], Sha Yang[1], Jiaojiao Bian[1], Ying Zhang[1], Yuquan Wang[2], Zhan Lv[2]

[1]Department of Pharmacy, North Sichuan Medical College, Nanchong 637000, Sichuan, P. R. China; [2]Department of Cardiology, Affiliated Hospital of North Sichuan Medical College, Nanchong 637000, Sichuan, P. R. China

Received April 23, 2024; Accepted May 15, 2024; Epub June 15, 2024; Published June 30, 2024

Abstract: Objective: To identify key genes associated with tumor-associated macrophages (TAMs), tumor immunotherapy, in the prognosis of lung adenocarcinoma (LUAD). Methods: The mRNA expression profiles of LUAD samples were obtained from The Cancer Genome Atlas (TCGA) database. The "CIBERSORT" R package was employed to calculate the proportion of innate immune cell infiltration in both tumor and adjacent normal tissues. TAM-associated genes in LUAD were identified to construct a prognostic risk model using weighted gene correlation network analysis (WGCNA), Least Absolute Shrinkage and Selection Operator (LASSO), and multivariate Cox regression analyses (COX). The IMvigor210 cohort was utilized to validate the roles of these genes as predictors of immunotherapy response. Tissue microarrays, immunofluorescence staining, and mRNA level detection methods were used to determine the correlation of risk factors in LUAD tissues. Results: CIBERSORT analysis revealed significant differences in innate immune cells between tumor and adjacent tissues. Seventy-four differential genes linked to these cells were identified from WGCNA. Four hub genes (endothelin receptor type B, vascular endothelial growth factor D (VEGFD), latent transforming growth factor beta binding protein 4 (LTBP4), and fibroblast growth factor receptor 4 (FGFR4)) in the TAM prognostic model were identified as independent prognostic risk factors ($P < 0.05$). VEGFD expression was identified as a low-risk factor for LUAD prognosis prediction ($P < 0.05$). Moreover, low-risk patients exhibited higher sensitivity to anti-PD-L1 therapy compared to high-risk patients ($P < 0.05$). VEGFD levels were negatively correlated with programmed cell death 1 (PD-1) levels ($r = -0.363$; $P < 0.05$), suggesting that VEGFD may serve as a predictor for anti-PD-1 treatment. Conclusions: VEGFD is associated with innate immunity in LUAD, it can predict LUAD prognosis, and therefor may be a potential predictor for anti-PD-1 treatment in patients with LUAD.

Keywords: Lung adenocarcinoma, tumor microenvironment, immunotherapy, VEGFD, PD-L1

Introduction

Lung cancer is a common malignant tumor worldwide, with the highest mortality among all cancers [1]. Non-small cell lung cancer (NSCLC) accounts for 85% of lung cancer cases, of which 50% are adenocarcinoma (LUAD) [2]. The 5-year survival rate for patients with advanced NSCLC is only 0-10% [3].

In recent years, in addition to traditional treatments for NSCLC such as chemotherapy, radiotherapy, and immunotherapy, several targeted and immunotherapeutic drugs have been employed for advanced NSCLC treatment [2]. Immune checkpoint inhibitors are the most common immunotherapeutic drugs used in cancer treatment, and their effectiveness is primarily influenced by immune cells infiltrating the tumor microenvironment (TME) [4]. The TME is closely associated with tumorigenesis, development, and metastasis, with innate immunity playing a major role in tumor immunotherapy [5]. Macrophages, key innate immune cells, exhibit different biological functions depending on the tumor's pathological stage. In the early stages of tumorigenesis, macrophages phagocytize tumor cells and present antigens that induce T cell immunity to inhibit tumor growth. However, in advanced tumors, macrophages promote tumor immune and drug resistance by upregulating immune checkpoint ligands (programmed cell death ligand 1 (PD-L1), programmed cell death ligand-2 (PD-L2), and B7-1) and cytokines related to tumor immunotherapy [6, 7].

https://doi.org/10.62347/OXRO7113

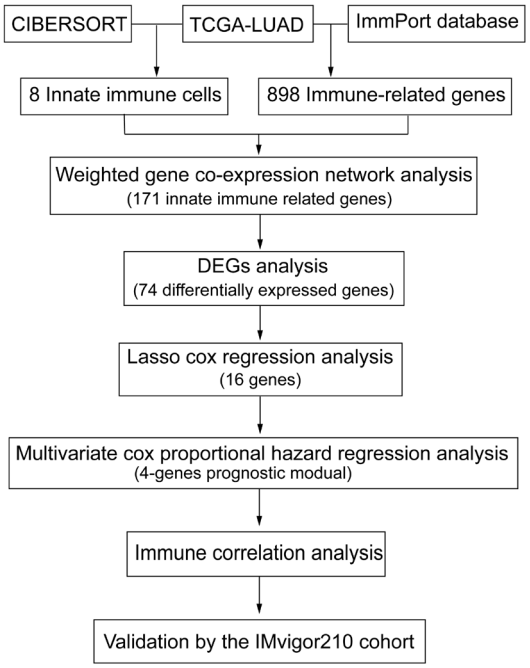

Figure 1. The bioinformatics analysis flowchart. Note: TCGA, The Cancer Genome Atlas Program; LUAD, Lung Adenocarcinoma; DEGs, differentially expressed genes; LASSO, Least Absolute Shrinkage and Selection Operator.

Many genes expressed in immune and tumor cells regulate immune cell function during tumorigenesis and progression. Tumor-associated macrophages (TAMs) are recruited to tumor tissues by colony-stimulating factor 1 (CSF1) [8]. Programmed cell death protein 1 (PD-1), expressed in T cells, reduces the cytotoxicity and activity of T cells toward tumor cells by binding to PD-L1 or PD-L2 on tumor cells [9]. Based on these mechanisms, immunotherapy, particularly immune checkpoint therapy, has made significant progress in clinical treatment. Unfortunately, immune checkpoint therapy can be ineffective and have adverse effects in some patients, influenced by genes related to immunotherapy. Therefore, identifying biomarkers to predict the efficacy of immune checkpoint inhibitors in specific patients is crucial [10, 11].

In this study, we identified key genes linked to TAMs, tumor immune therapy, and their association with the prognosis of LUAD. Data mining was performed using the TCGA database with several analytical approaches, including weighted gene correlation network analysis (WGCNA), GSVA, and the "CIBERSORT" R package. The IMvigor210 cohort was used to identify potential immunotherapy biomarkers in patients with LUAD. The workflow chart is shown in **Figure 1**.

Methods

Acquiring and processing the transcriptome expression and clinical data of LUAD

First, LUAD RNA sequencing profiles and information were obtained from the TCGA database, including 468 LUAD tissues and 58 adjacent non-tumor samples. Excluding samples with incomplete information or short survival time (< 1 month), an effective sample size of 513 remained. Genes associated with immunity were acquired from the ImmPort database, and 898 genes were analyzed using WGCNA after gene intersection in the expression data.

Evaluation of the immune infiltration component of TME

The "CIBERSORT" (R, version 4.0.2) was used to predict the immune infiltration fraction matrix based on the expression matrix, to analyze the clinical significance of infiltrating immune cells. The abundance of immune cells in the LUAD immune microenvironment was first calculated. The different proportions of infiltrating innate immune cells between tumor and adjacent tissues were analyzed using a two-sided t-test.

Construction of co-expression network of the immune infiltration

First, WGCNA was used to construct gene modules related to infiltrating immune cells and clinical features. The samples were clustered based on the LUAD immune gene expression matrix to detect outliers. After removing outliers, the "FlashClust" package was used to stratify the remaining samples and explore the relationships between them. The features of each sample were converted into different colors: white indicated low, red indicated high, and gray indicated missing entries. In WGCNA, the soft threshold is a key parameter used to determine the strength of the network connectivity. The soft threshold was set based on the scale-free topological fit index, and a value above 0.85 was selected. Finally, we set the soft

threshold to 3 to construct the weighted adjacency matrix and topological overlap matrix (TOM) (cutting height = 0.25, minimum module size = 30), dividing the genes into various modules.

Determination of the correlation between modules and clinical traits

The eigengene module was used to define the principal components of each gene module. Gene significance, calculated as the absolute value of the correlation between gene profiles and clinical traits, was used to assess this relationship. Module membership was defined as the correlation between gene profiles and the eigengene of each module. The Pearson correlation coefficient was then calculated to estimate the module significance of the eigengene module and infiltrating innate immune cells. A module was considered significantly associated with innate immune cells when $|P| < 0.05$.

Analysis of differential expression of immune genes

The degree of gene connectivity was further analyzed using Cytoscape. Differentially expressed genes (DEGs) between tumor and adjacent non-tumor samples were determined E the "DESeq2" package. Immune genes satisfying both |log2foldchange| > 1 and adjusted P < 0.05 were considered DEGs and were visualized using the "EnhancedVolcano" R package.

GO and GSVA

Gene ontology (GO) analysis was performed on immune DEGs, with adjusted P < 0.01 considered statistically significant. Gene Set Variation Analysis (GSVA) was used to identify significant pathways among patients with different risk scores (RS) (high and low). The gene sets were obtained from the MSigDB database, with statistical significance defined as a false discovery rate (FDR) < 0.05.

Analysis of prognostic signature of immune DEGs

LASSO was used to reduce dimensionality and establish the risk score (RS) for the most robust markers. To avoid model overfitting, lambda. min (λ) was determined as the optimal value of the parameter using 10-fold cross-validation. COX regression analysis was employed to select essential prognostic markers of LUAD and construct an RS module. The calculation formula was as follows:

$$Risk\ score = \sum_{i=1}^{n} Cofficient_i \times Expression_i$$

The diagnostic capacity of the module was assessed using Kaplan-Meier survival (KM) analysis and a time-dependent receiver operating characteristic (ROC) curve. The module's independent predictive ability for LUAD, considering multiple clinical characteristics (gender, age, and tumor stage), was analyzed using COX regression. The Wilcoxon test was performed to estimate the difference in infiltrating immune cells between the two risk groups ($P < 0.05$).

Human samples and tissue microarrays (TMAs)

LUAD tissues and matched para-carcinoma tissues (30 pairs) were collected from the Affiliated Hospital of North Sichuan Medical College, with approval of the Ethics Committee, number 2020 ER063-2. These tissues were fixed in 4% paraformaldehyde overnight. The paraffin blocks were processed using an automatic TMA production instrument (TMA Master, 3DHISTECH). The sampling points and microarray graphics were set, and the system automatically completed steps such as drilling, sampling, and core injection. Para-carcinoma tissues were placed in rows 1-3, and corresponding matched tumor tissues were placed in rows 4-6.

Immunofluorescence (IF) staining

The TMA chip was incubated at 60°C for 4 hours, followed by dewaxing, dehydration, treatment with 3% hydrogen peroxide, heat-induced antigen retrieval, blocking with 3% BSA, permeabilization with 0.2% Triton X-100, and co-incubation with antibodies against vascular endothelial growth factor D (VEGFD) (1:200, R6074, Zenbio), PD-1 (1:400, 66220-1-1g, Proteintech), and CD86-APC (1:200, 17-0869-42, eBioscience) overnight at 4°C. The secondary antibodies, FITC-labelled anti-mouse IgG (1:150, A0568, Beyotime) and Cy3-labelled anti-rabbit IgG (1:150, A0516, Beyotime), were then applied. Images were obtained using a microscope (VS200, Olympus, Japan).

Table 1. The primers used for Real-time quantitative polymerase chain reaction

Gene	Forward	Reverse
VEGFD	ACGGATACAGCTAGTGTTTGACA	GTCCACACCATCGTCCTCTAATA
PD-1	CCAGGATGGTTCTTAGACTCCC	TTTAGCACGAAGCTCTCCGAT

Note: VEGFD, vascular endothelial growth factor D; PD-1, Programmed cell death 1.

RT-qPCR

RNA was extracted using the Trizol kit, and complementary DNA (cDNA) was synthesized with the cDNA Synthesis Kit (R211-01, Vazyme). Quantification was performed using SYBR Green (Bio-Rad). GAPDH was used as the internal control for RT-qPCR. Sequences of primers for VEGFD and PD1 are listed in **Table 1**.

Statistical analysis

The statistical software used in this study was GraphPad Prism 9. Quantitative data were presented as mean ± standard deviation and analyzed by paired two-tailed t-test. Qualitative data were presented as n (%) and analyzed using the chi-square test. A *P*-value < 0.05 was considered statistically significant.

Results

Innate immune cell infiltration in the tumor immune microenvironment

The landscape of 10 innate immune cells in LUAD tissues was evaluated using CIBERSORT software, showing that macrophages had the highest proportion of innate immune-infiltrating cells (**Figure 2A**). We also compared the proportions of innate immune cells between normal and tumor tissues. The infiltration of M2 macrophages, monocytes, and resting NK cells was decreased in tumor tissues, while the infiltration of M1 macrophages and activated NK cells was increased (P < 0.05) (**Figure 2B**).

Weighted co-expression network construction associated with infiltrating immunity cells

To explore the role of innate immune cells in LUAD, a hierarchical clustering dendrogram of 513 LUAD samples was constructed, and 18 samples were excluded based on a Euclidean distance of 7000 (**Figure 3A**). Tumor-associated immune cell information, including that of the 10 innate immune cells, was attached to the cluster (**Figure 3B**). According to the scale-free topology model fit, the scale-free topological fit index was 0.85, and the soft threshold was set to 3 (**Figure 3C**). The co-expressed modules, comprising six total modules, are shown in **Figure 3D**. For further analysis, the top three modules with the highest correlations (brown, turquoise, and green) were selected (P < 0.05) (**Figure 3E**). The brown module showed a positive correlation with M1 macrophages (r = 0.43) but a negative correlation with M2 macrophages (r = -0.12). The turquoise module presented a positive correlation with both M1 and M2 cells (r = 0.13, 0.28), and the green module showed a positive correlation with M2 macrophages (r = 0.16) and a negative correlation with M1 macrophages (r = -0.10). There were 128, 38, and 100 hub genes in these three modules, respectively, for further analyses.

Protein-protein interaction networks and pathways analysis for hub genes associated with immune cells

Cytoscape was used to construct protein-protein interaction networks for the genes in the brown, green, and turquoise modules to screen out hub genes (**Figure 4A-C**). The volcano plot of these genes identified 74 DEGs, including four downregulated genes such as endothelin receptor type B (EDNRB) and VEGFD (P < 0.05) (**Figure 4D**). Additionally, functional enrichment analysis revealed that these genes were significantly involved in biological processes related to tumor immunity, including leukocyte proliferation and migration, myeloid leukocyte migration, regulation of chemotaxis, immune receptor activity, and receptor-ligand activity (**Figure 4E**).

Construction of prognostic risk model based on DEGs

A prognostic model was constructed using LASSO regression. Sixteen genes were found to be correlated with LUAD prognosis (**Figure 5A**, **5B**). The calculation formula for the RS of the prognostic model is as follows: RS = 0.0057 × *FGFR4* + 0.1575 × *TNFAIP3* - 0.1406 × *VIPR1* - 0.0526 × *ADA2* + 0.0324 × *EDNRB* + 0.0475 ×

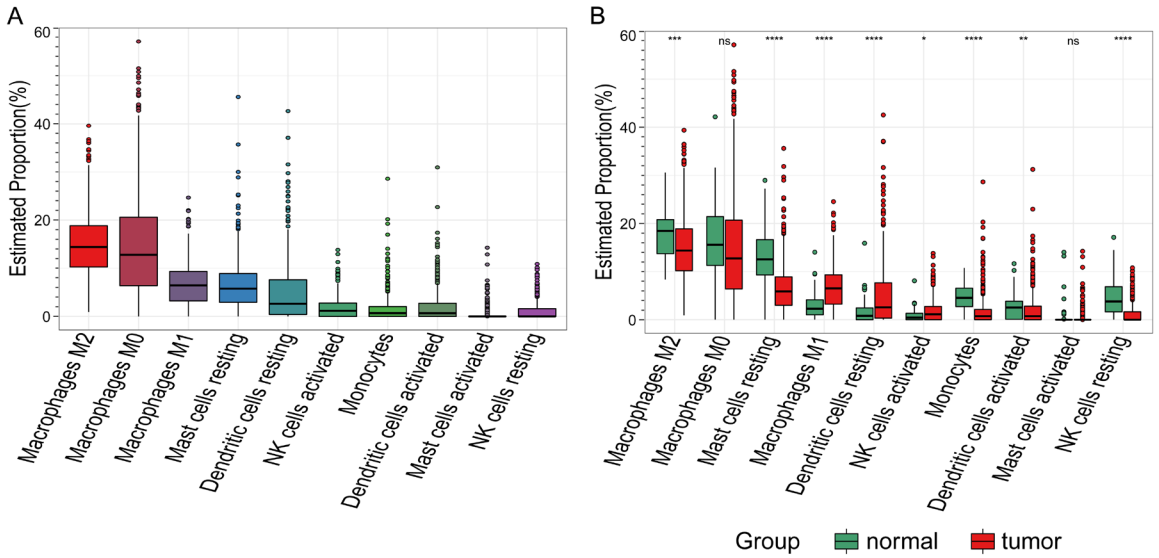

Figure 2. Analysis of innate immune infiltration in lung adenocarcinoma (LUAD) and adjacent normal tissues. A. The proportion of infiltration of 10 innate immune cell types in the tumor groups. B. Differences in innate immune cell infiltration between LUAD and adjacent normal tissues. The proportion of infiltration between LUAD and adjacent normal groups was analyzed using a two-sided t-test. *P*-value significance codes: * < 0.05; ** < 0.01; *** < 0.001; **** < 0.0001.

NPR1 - 0.0532 × *CD79A* - 0.0586 × *BTK* + 0.0136 × *SLIT2* - 0.0849 × *IL5RA* - 0.0498 × *VEGFD* - 0.0038 × *PTGDS* + 0.0989 × *LTBP4* - 0.0395 × *AGER* + 0.0331 × *SEMA5A*.

The time-dependent ROC curve was used to evaluate the accuracy of the prognostic model. The area under the curve (AUC) for this model at 1, 3, and 5 years were 0.699, 0.721, and 0.711, respectively, suggesting that this model accurately predicts LUAD prognosis (**Figure 5C**). Kaplan-Meier curves indicated a lower survival rate in high-risk (HR) patients compared to low-risk (LR) patients (**Figure 5D**) ($P < 0.05$).

Four genes were determined as independent prognostic factors in LUAD

Four genes from the sixteen identified were determined to be independent risk factors for LUAD prognosis (**Figure 6A**). The RS was defined by the regression coefficient: RS = 0.2845 × *EDNRB* - 0.4562 × *VEGFD* + 0.2363 × *LTBP4* + 0.1784 × *FGFR4*. Patients were divided into HR and LR groups according to the median risk score. The survival time of the low-risk patients was significantly longer ($P < 0.05$, **Figure 6B**). The distribution of RS and the expression levels of the four hub genes in LUAD patients are shown in **Figure 6C**. The levels of Fibroblast growth factor receptor 4 (FGFR4), Latent transforming growth factor beta binding protein 4 (LTBP4), and EDNRB were higher in the HR group compared to the LR group, while the expression of VEGFD was decreased. A higher proportion of patients in the HR group died compared to those in the LR group. Clinical parameters of LUAD patients, including gender, age, TNM stage, and smoking status, were used as independent variables. Age, clinical stage, smoking status, and risk score were confirmed as independent risk factors by COX regression (**Figure 6D**). GSVA analysis suggested that the four risk factors were involved in pathways linked to multicancer invasiveness signatures, the prognosis of multiple tumors such as thyroid, colorectal, and breast cancers, and leukotriene biosynthetic processes (**Figure 6E**).

Four independent risk genes as predictors for immunotherapy treatment in patients with LAUD

The risk score was used to assess the prognostic value of immunotherapy treatment in LUAD based on FGFR4, LTBP4, EDNRB, and VEGFD. Patients who responded to anti-PD-L1 treatment exhibited low-risk scores for FGFR4, LTBP4, EDNRB, and VEGFD, whereas patients who did not respond to anti-PD-L1 treatment had high-risk scores for these four genes

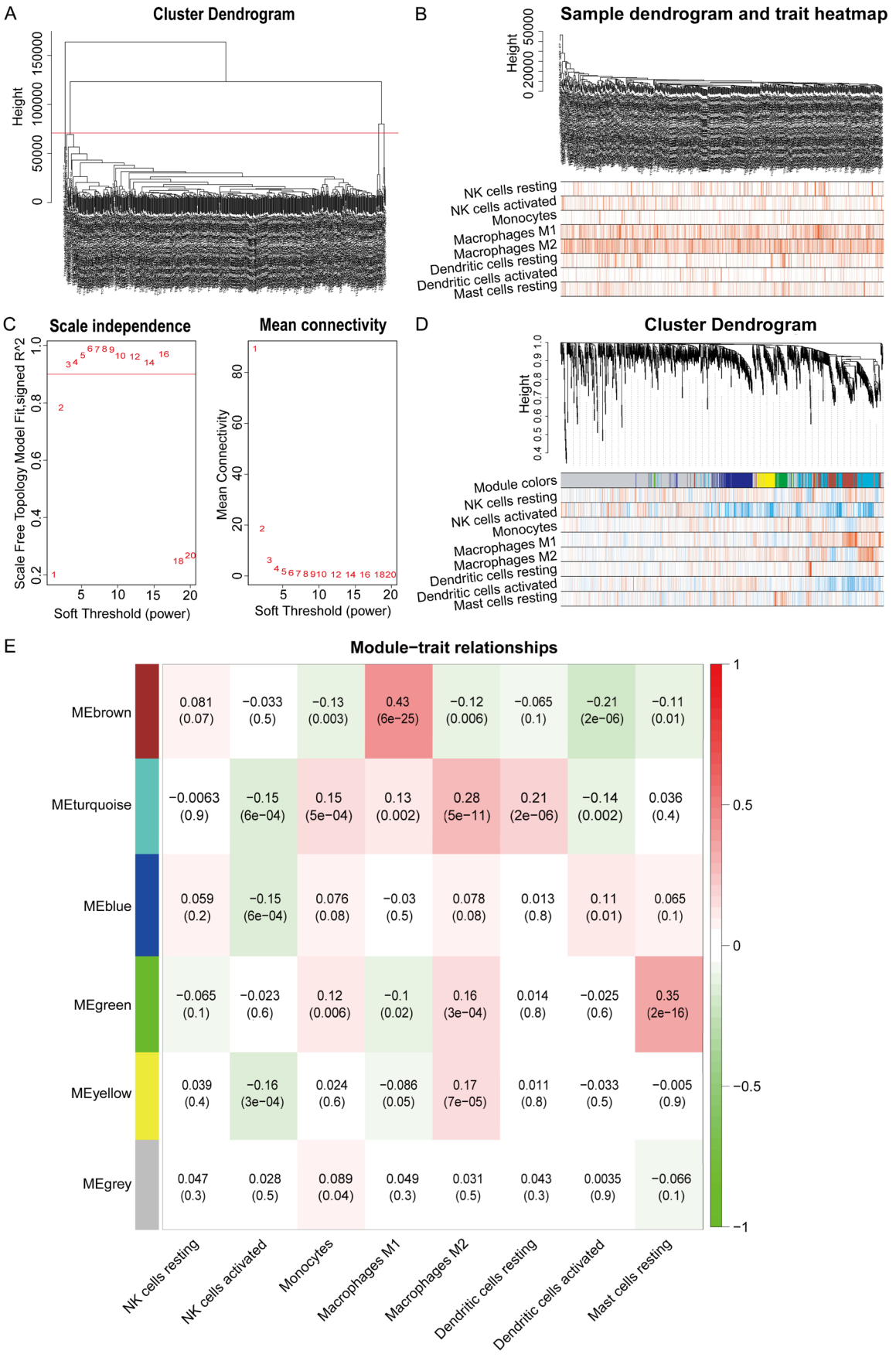
A
Cluster Dendrogram
Height
B
Sample dendrogram and trait heatmap
NK cells resting
NK cells activated
Monocytes
Macrophages M1
Macrophages M2
Dendritic cells resting
Dendritic cells activated
Mast cells resting
C
Scale independence
Scale Free Topology Model Fit,signed R^2
Soft Threshold (power)
Mean connectivity
Mean Connectivity
Soft Threshold (power)
D
Cluster Dendrogram
Height
Module colors
E
Module−trait relationships
MEbrown
MEturquoise
MEblue
MEgreen
MEyellow
MEgrey
0.081 (0.07)
−0.033 (0.5)
−0.13 (0.003)
0.43 (6e−25)
−0.12 (0.006)
−0.065 (0.1)
−0.21 (2e−06)
−0.11 (0.01)
−0.0063 (0.9)
−0.15 (6e−04)
0.15 (5e−04)
0.13 (0.002)
0.28 (5e−11)
0.21 (2e−06)
−0.14 (0.002)
0.036 (0.4)
0.059 (0.2)
−0.15 (6e−04)
0.076 (0.08)
−0.03 (0.5)
0.078 (0.08)
0.013 (0.8)
0.11 (0.01)
0.065 (0.1)
−0.065 (0.1)
−0.023 (0.6)
0.12 (0.006)
−0.1 (0.02)
0.16 (3e−04)
0.014 (0.8)
−0.025 (0.6)
0.35 (2e−16)
0.039 (0.4)
−0.16 (3e−04)
0.024 (0.6)
−0.086 (0.05)
0.17 (7e−05)
0.011 (0.8)
−0.033 (0.5)
−0.005 (0.9)
0.047 (0.3)
0.028 (0.5)
0.089 (0.04)
0.049 (0.3)
0.031 (0.5)
0.043 (0.3)
0.0035 (0.9)
−0.066 (0.1)
NK cells resting
NK cells activated
Monocytes
Macrophages M1
Macrophages M2
Dendritic cells resting
Dendritic cells activated
Mast cells resting

Figure 3. Weighted gene co-expression network analysis (WGCNA) and identification of significant modules. A. Outlier samples were detected using a clustering dendrogram. B. Sample dendrogram and trait heatmap. Each color represents the trait of each sample in the heatmap: white indicates low, red indicates high, and grey indicates a missing entry. C. Identification of the soft threshold power for WGCNA. The scale-free fitting index was analyzed for diverse soft-threshold powers (β). The power of β = 3 was selected as the soft threshold. D. Dendrogram of the immune genes clustered by topological overlaps. E. Heatmap showing the correlation between modules and immune cells. The red module represents a positive correlation with clinical traits, while the green module represents a negative correlation.

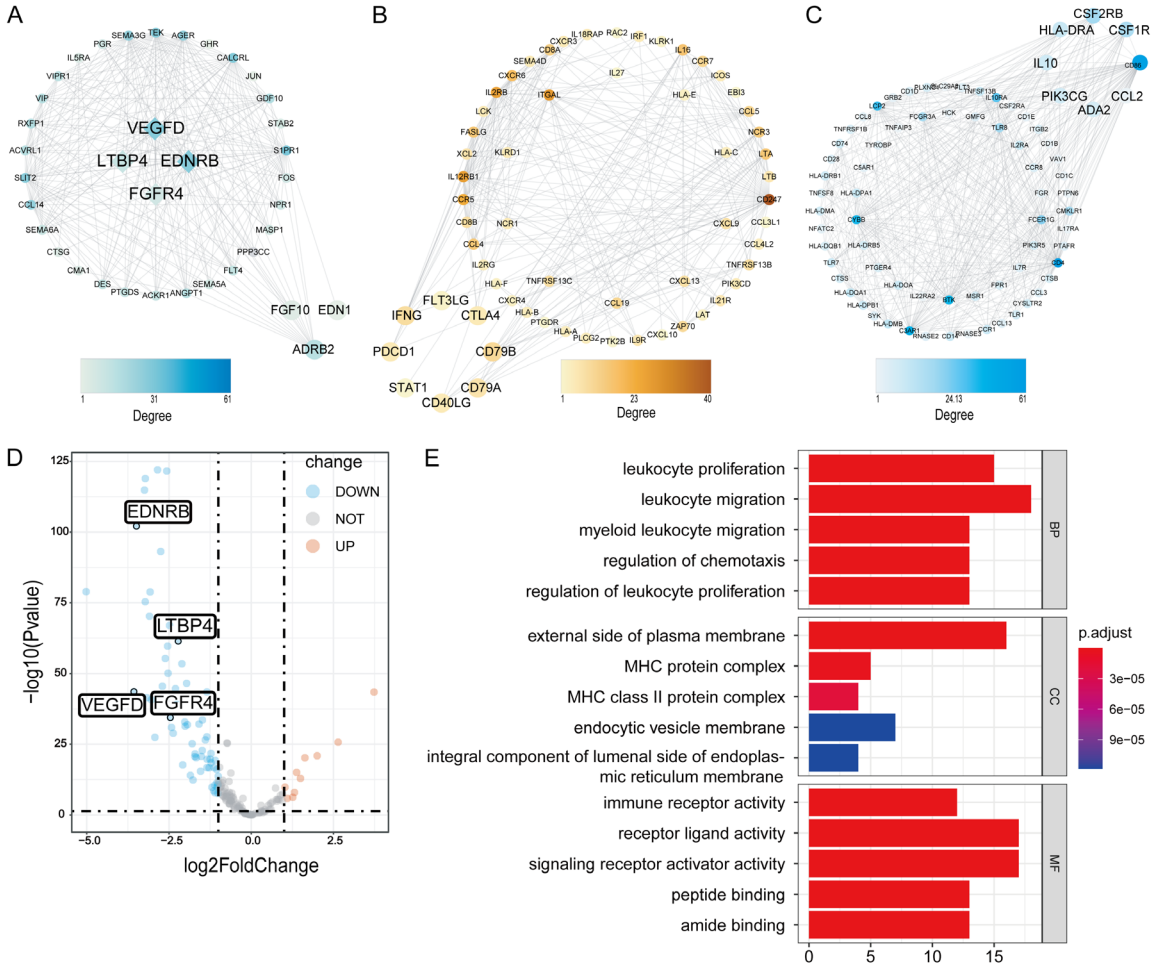

Figure 4. Exploration of differentially expressed genes (DEGs). Protein-protein interaction networks of immune genes in (A) brown, (B) green, and (C) turquoise modules. (D) Volcano plot of DEGs screened based on three modular genes. (E) Gene Ontology (GO) enrichment analysis of immune DEGs.

(**Figure 7A**). Twenty-nine percent of patients with a low RS responded to anti-PD-L1 treatment, which was higher than the response rate in the LR group (**Figure 7B**). Furthermore, the KM curve showed that patients with low RS had significantly prolonged survival times (**Figure 7C**).

Additionally, Pearson's correlation analysis showed that *EDNRB and VEGFD* levels were positively correlated with M2 macrophages (r = 0.20, 0.15; $P < 0.05$) and negatively associated with M0 macrophages (r = -0.25, -0.30; $P < 0.05$) (**Figure 7D**). The correlation between the expression changes of the four genes and different immune checkpoints was also analyzed. As shown in **Figure 7E**, *EDNRB* and *VEGFD* expressions were positively correlated with PD-L1, PD-L2, TIM3, and CD96, but negatively correlated with TIGIT, CTLA4, LAG3, and PD-1.

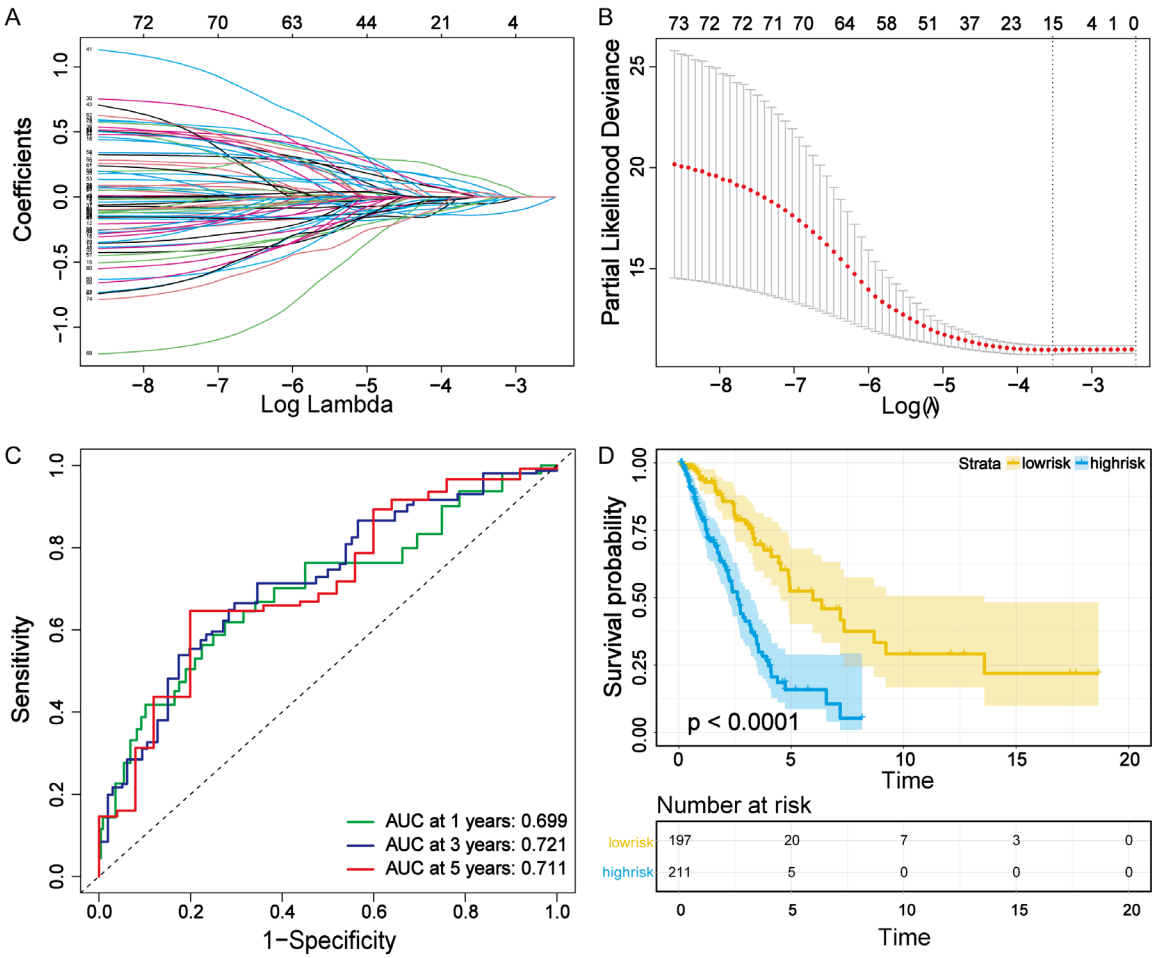

Figure 5. Immune risk model constructed by Least Absolute Shrinkage and Selection Operator (LASSO) Cox regression analysis. A. Regression coefficients of 74 genes determined by LASSO Cox regression analysis. B. Identification of suitable parameters (λ). The two vertical lines represent lambda.min (the value of λ that gives the minimum mean cross-validated error) and lambda.1 se (the value of λ that gives the most regularized model such that the cross-validated error is within one standard error of the minimum). C. Time-dependent receiver operating characteristic (ROC) curve evaluating the prognostic values of the risk score. D. Kaplan-Meier curves showing the overall survival of lung adenocarcinoma (LUAD) patients in low- and high-risk groups.

LTBP4 was positively correlated with PD-L1, PD-L2, TIM3, and CD96, while *FGFR4* was negatively correlated with LAG3, CTLA4, and TIGIT ($P < 0.05$).

TMA, RT-qPCR, and immunofluorescence staining indicated that VEGFD expression was negatively correlated with PD-1 levels in LUAD tissues at both mRNA and protein levels (**Figure 8A-C**). The correlation coefficient between VEGFD and PD-1 at the mRNA level was -0.363 (P = 0.005). The expression levels of VEGFD and PD-1 were significantly related to tumor stage (r = -0.463, 0.617; P < 0.05; **Table 2**). Patients with low *VEGFD* levels had worse prognoses, whereas patients with high *VEGFD* expression showed better prognoses (**Figure 8D**, $P < 0.05$). However, different PD-1 levels did not significantly impact patient prognosis (**Figure 8E**).

Discussion

Multiple cell types, including TAMs, in TME can influence tumor cell proliferation and response to chemotherapy by secreting cytokines, chemokines, and other factors [5, 12]. This study analyzes TAM hub genes related to the immunotherapy of LUAD and their relationship with prognosis, aiming to provide new biomarkers for LUAD patient immunotherapy.

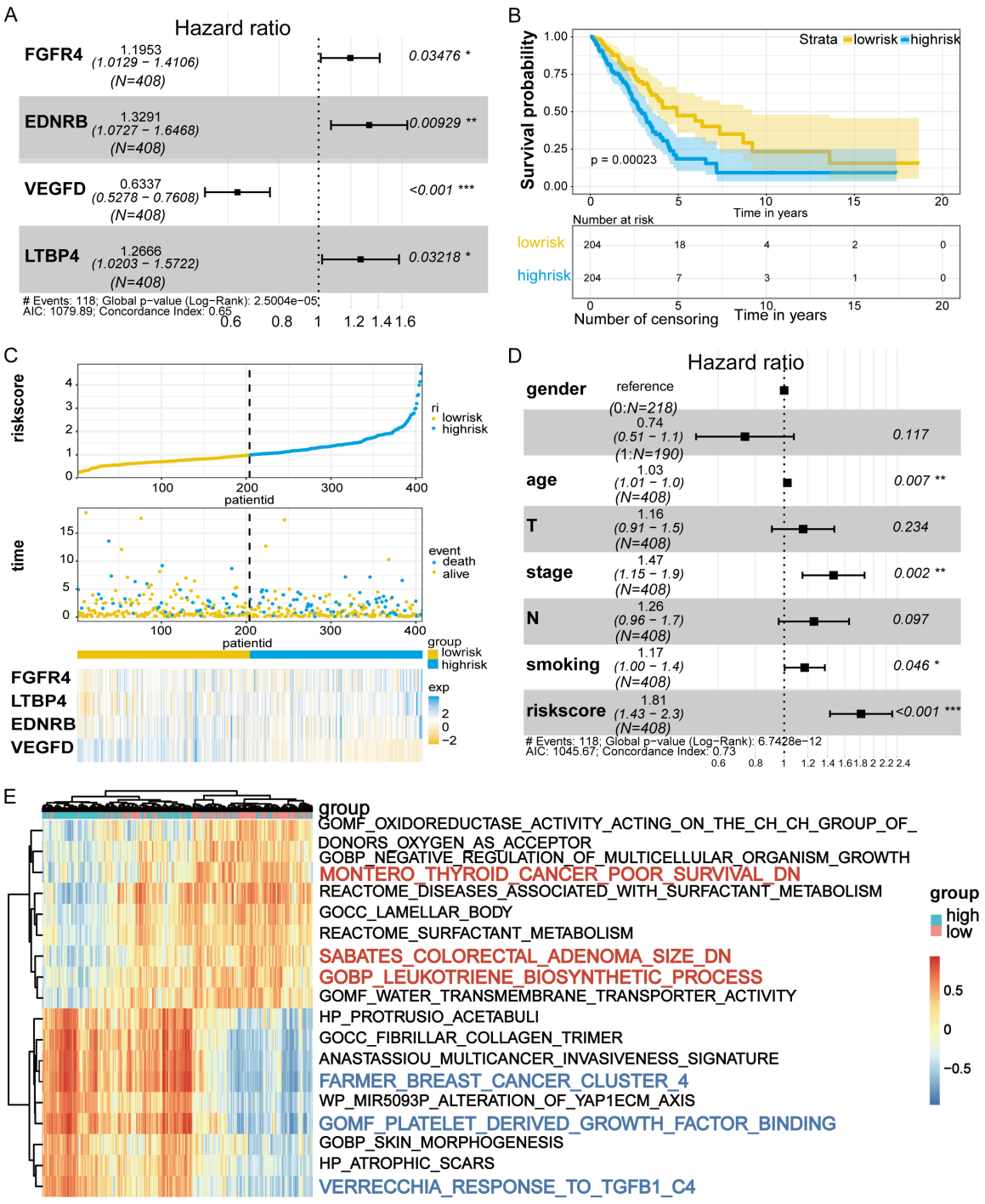

Figure 6. Multivariate stepwise Cox regression analysis used to establish prognostic genes. A. Forest plot of the multivariate Cox regression analysis. B. Kaplan-Meier plot of the risk score. C. Distribution of risk score, survival status, and hub immune gene expression profiles of each patient with lung adenocarcinoma (LUAD). D. Multivariate Cox analysis of the risk score and other clinical prognostic traits of patients with LUAD. E. Gene set variation analysis (GSVA) enriched different signaling pathways based on high- and low-risk groups. Genes include fibroblast growth factor 4 (FGFR4), endothelin receptor type B (EDNRB), vascular endothelial growth factor D (VEGFD), and latent-transforming growth factor beta-binding protein 4 (LTBP4).

WGCNA provides a comprehensive method to study the correlation between gene profiles and clinical phenotypes and has been widely used to screen therapeutic and prognostic bio-

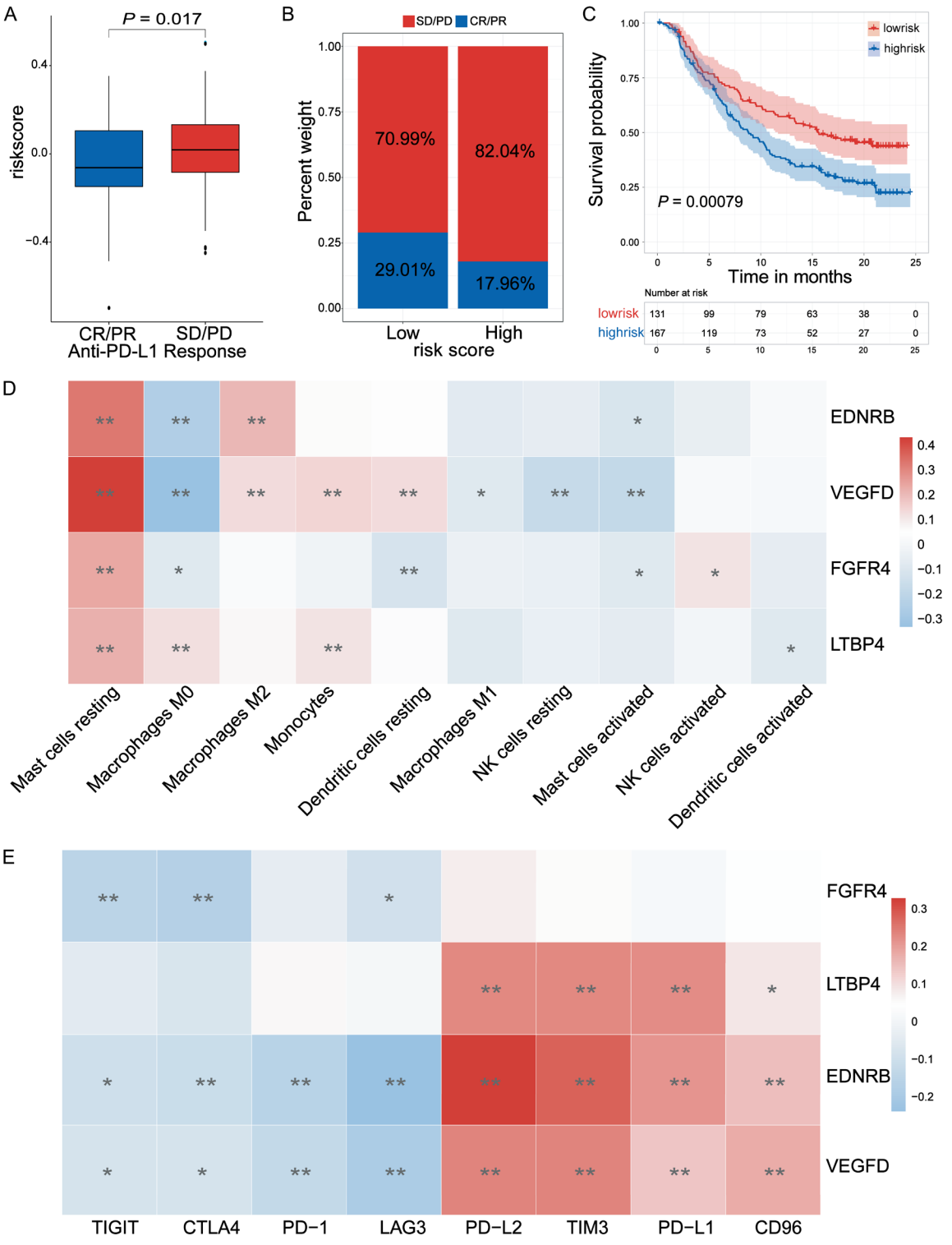

Figure 7. Predictors of the four hub genes for immunotherapy treatment. A. Comparison of risk scores in different anti-PD-L1 clinical response groups of the IMvigor210 cohort (complete response [CR]/partial response [PR] and stable disease [SD]/progressive disease [PD]). B. Treatment response rate to PD-L1 blockade therapy in high- and low-risk groups of the IMvigor210 cohort. C. Kaplan-Meier survival curves for high- and low-risk patients in the IMvigor210 cohort. D. Correlation between the four hub genes and innate immune infiltrating cells. E. Correlation between the four hub genes and immune checkpoints (*P < 0.05; **P < 0.01). The four hub genes are fibroblast growth factor 4 (FGFR4), endothelin receptor type B (EDNRB), vascular endothelial growth factor D (VEGFD), and latent-transforming growth factor beta-binding protein 4 (LTBP4).

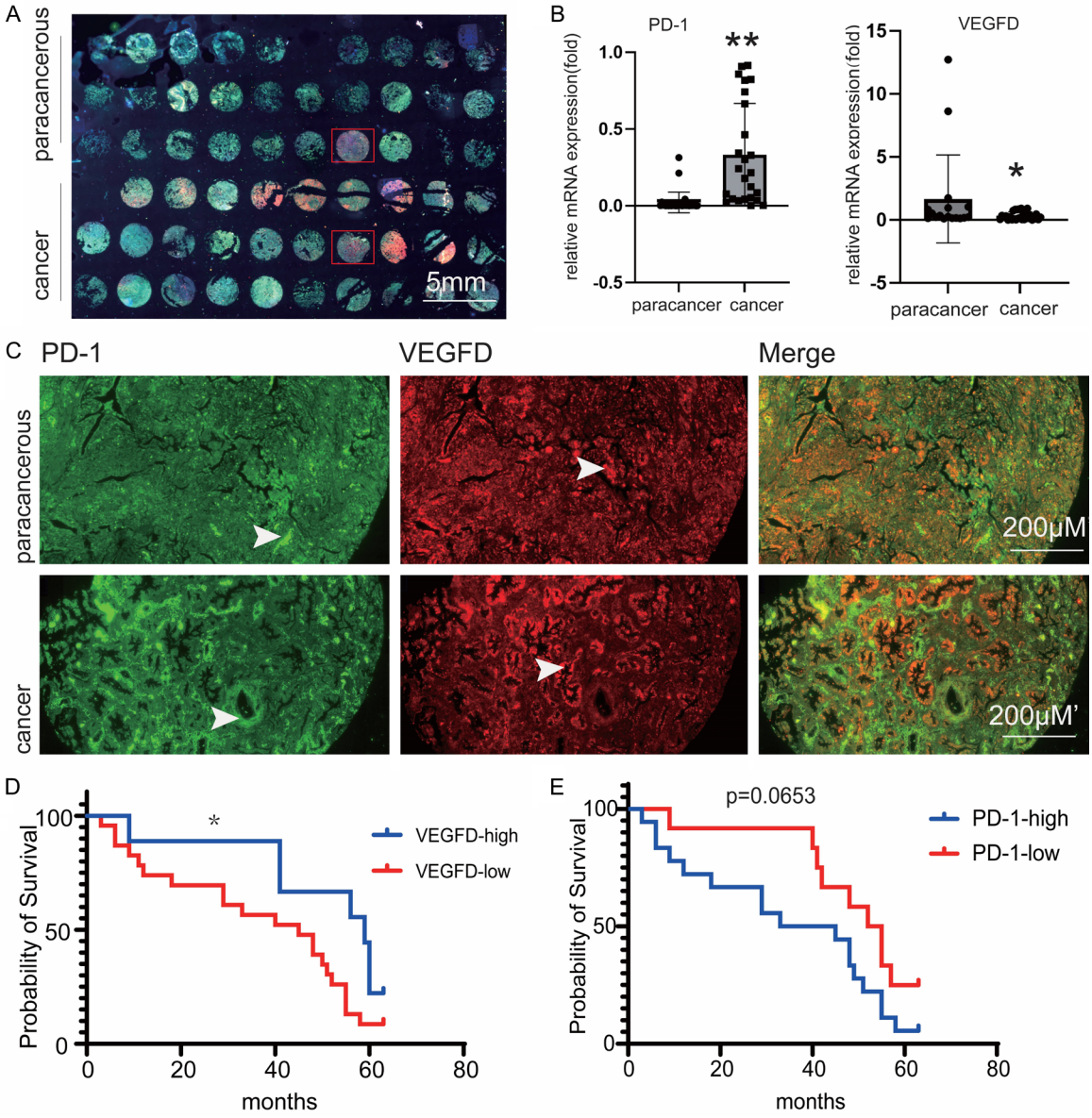

Figure 8. Expression levels of VEGFD and PD-1 and their prognostic relationship in LUAD tissues. A. Tissue microarrays of LUAD and matched para-carcinoma were co-stained with VEGFD and PD-1. B. VEGFD and PD-1 expression in LUAD at the mRNA level (n = 30). Data are represented as "Mean with SEM", *P < 0.05 (unpaired two-tailed t-test). C. Immunofluorescence staining for VEGFD and PD-1 in LUAD and matched para-carcinoma. D. Probability of patient survival based on varying levels of VEGFD (*P < 0.05, log-rank test). E. Probability of patient survival based on varying levels of PD-1 expression. VEGFD, vascular endothelial growth factor D; PD-1, programmed cell death 1; LUAD, lung adenocarcinoma.

markers for many complex diseases [13-16]. In this study, a TAM-related gene prognosis model in LUAD was established using WGCNA and CIBERSORT, and further combined with LASSO Cox regression and Cox proportional hazard regression analyses to identify prognostic and immunotherapy-related gene markers (FGFR4, LTBP4, EDNRB, and VEGFD). These hub genes were validated using the IMvigor210 cohort. The genes obtained from these analyses are highly reliable for predicting prognosis and immune treatment in LUAD.

Innate immunity plays a crucial role in tumor immunity and immunotherapy [5]. It is well known that M1 macrophages act as pro-inflammatory cells by secreting interleukins and pro-inflammatory chemokines in diseases, where-

Table 2. The correlation between VEGFD, PD-1 expression and clinicopathological characteristics in LUAD patients

Clinicopathological characteristics	Total	VEGFD expression		χ^2	P	PD-1 expression		χ^2	P
		High	Low			High	Low		
Age (y)				0.130	0.719			0.028	0.866
> 65	8	2 (25.00)	6 (75.00)			5 (62.50)	3 (37.50)		
≤ 65	22	7 (31.82)	15 (68.18)			13 (59.09)	9 (40.91)		
Gender				0.730	0.543			1.693	0.193
Female	9	2 (22.22)	7 (77.78)			7 (77.78)	2 (22.22)		
Male	21	7 (33.33)	14 (66.67)			11 (52.38)	10 (47.62)		
Smoking				0.106	0.475			0.238	0.626
Yes	12	4 (33.33)	8 (66.67)			9 (75.00)	3 (25.00)		
No	18	5 (27.78)	13 (72.22)			12 (66.67)	6 (33.33)		
TNM stage				6.429	0.011			11.429	0.001
I	10	6 (60.00)	4 (40.00)			3 (30.00)	7 (70.00)		
II/III	20	3 (15.00)	17 (85.00)			18 (90.00)	2 (10.00)		

Note: VEGFD, Vascular Endothelial Growth Factor D; PD-1, Programmed cell death 1; LUAD, Lung Adenocarcinoma; TNM, Tumor Node Metastasis.

as M2 macrophages secrete cytokines and chemokines to exert anti-inflammatory functions [17, 18]. In this study, an increase in M1 macrophages and a decrease in M0 and M2 macrophages were observed, indicating that the immune balance in patients was disrupted. This imbalance may promote tumor cell metastasis and evasion of immune clearance and surveillance, ultimately affecting patient prognosis [6, 7].

There is heterogeneity between tumor and para-cancerous tissues; high infiltration of M1 macrophages in NSCLC indicates a better prognosis for patients, whereas an increase in M2 macrophages indicates a poor prognosis [17]. Therefore, macrophage-linked genes may affect the prognosis of LUAD [18]. In this study, WGCNA, CIBERSORT, and a series of bioinformatics analyses identified immune cell-related genes EDNRB, VEGFD, LTBP4, and FGFR4 as independent risk factors for LUAD prognosis. The risk score prediction model established based on these four genes can effectively distinguish between high- and low-risk populations with poor prognosis. VEGFD was confirmed as a protective gene, whereas EDNRB, LTBP4, and FGFR4 were risk factors for LUAD. These results are consistent with previous reports that high expression of VEGFD in LUAD is beneficial for patient prognosis [19-21]. FGFR4 is an oncogene that can be acquired through genetic mutations in human cancers, contributing to tumor proliferation, migration, angiogenesis, and resistance to anti-neoplastic agents [22, 23]. LD-1, a monoclonal antibody targeting FGFR4, has been used in clinical trials for hepatocellular carcinoma treatment [24, 25]. Additionally, EDNRB and LTBP4 are involved in functional vascularization, tumor metastasis, and prognosis [26-29]. The four genes were also negatively correlated with several innate immune cells, including M1 macrophages, but positively correlated with M2 macrophages, suggesting that these genes may directly or indirectly affect adaptive immunity through innate immunity.

The discovery of predictive biological targets for individualized therapies against tumor immune checkpoint inhibitors is a new strategy for tumor treatment [30]. Currently, several immune checkpoint inhibitors (anti-PD-1), such as atezolizumab, durvalumab, nivolumab, and pembrolizumab, are used as standard treatments for different stages of lung cancer.

Immune checkpoint inhibitors, particularly PD-1 and PD-L1 inhibitors, have become standard therapeutic drugs for malignancies such as NSCLC [31]. Patients can be treated with anti-PD-1 agents alone or in combination with chemotherapeutic drugs, depending on the PD-L1 expression of the tumor cells [32]. Bevacizumab, a monoclonal antibody targeting VEGFA, degrades the tumor vascular system. The Food and Drug Administration recommends bevacizumab combined with atezolizumab (an anti-PD-L1) as first-line chemotherapeutic agents in the treatment of LUAD [33]. Our data showed

that the four hub genes were significantly correlated with PD-1, PD-L1, and PD-L2, particularly VEGFD and EDNRB, which are closely associated with eight immune checkpoints. This suggests that the expression levels of these four genes may be potential mechanisms involved in checkpoint inhibitors, making them potential targets for LUAD immunotherapeutic agents. Clinical trials demonstrated an inverse relationship between the mRNA or protein level of VEGFD and the level of PD-1 in LUAD tissues from 30 patients with stage I-III LUAD. Survival analysis of these 30 patients showed that those with low VEGFD expression had a worse prognosis compared to those with high VEGFD expression. These results further demonstrate that VEGFD can be a predictor for LUAD prognosis and may be a potential predictor of anti-PD-1 therapy in LUAD patients. However, the small sample size is a limitation of this study, which may affect the significance of the statistical results of clinical trials. Therefore, future studies with larger samples are needed.

In summary, we screened and confirmed four hub genes related to innate immunity in LUAD, namely, EDNRB, VEGFD, LTBP4, and FGFR4. Our findings showed that VEGFD, which is related to innate immunity in LUAD, can be used to predict LUAD prognosis and may be a potential predictor of anti-PD-1 treatment for patients with LUAD.

Acknowledgements

We are grateful for the TCGA database and for the IMvigor210 cohort for the provision of free data. We give thanks to Xiangyu Pan (State Key Laboratory of Biotherapy) for his comprehensive guidance in algorithms and methods. This study was supported by the Project for the First-Class Pharmaceutical Sciences of North Sichuan Medical College (CBY21-YLXK03), the Project for the Natural Science of North Sichuan Medical College (CBY21-QA31), the Research and Development Program of Affiliated Hospital of North Sichuan Medical College (2022JC026), the National College Student Innovation and Entrepreneurship Training Program Project (202210634031), and the Health Department of Sichuan Province (21PJ188).

Disclosure of conflict of interest

None.

Address correspondence to: Drs. Yuquan Wang and Zhan Lv, Department of Cardiology, Affiliated Hospital of North Sichuan Medical College, Nanchong 637000, Sichuan, P. R. China. Tel: +86-0817-2598062; E-mail: wyq112379@163.com (YQW); lvzhan@nsmc.edu.cn (ZL)

References

[1] Sung H, Ferlay J, Siegel RL, Laversanne M, Soerjomataram I, Jemal A and Bray F. Global cancer statistics 2020: GLOBOCAN estimates of incidence and mortality worldwide for 36 cancers in 185 countries. CA Cancer J Clin 2021; 71: 209-249.

[2] Sun L, Bleiberg B, Hwang WT, Marmarelis ME, Langer CJ, Singh A, Cohen RB, Mamtani R and Aggarwal C. Association between duration of immunotherapy and overall survival in advanced non-small cell lung cancer. JAMA Oncol 2023; 9: 1075-1082.

[3] Li Y, Yan B and He S. Advances and challenges in the treatment of lung cancer. Biomed Pharmacother 2023; 169: 115891.

[4] Vornholz L, Isay SE, Kurgyis Z, Strobl DC, Loll P, Mosa MH, Luecken MD, Sterr M, Lickert H, Winter C, Greten FR, Farin HF, Theis FJ and Ruland J. Synthetic enforcement of STING signaling in cancer cells appropriates the immune microenvironment for checkpoint inhibitor therapy. Sci Adv 2023; 9: eadd8564.

[5] Hinshaw DC and Shevde LA. The tumor microenvironment innately modulates cancer progression. Cancer Res 2019; 79: 4557-4566.

[6] Anami T, Pan C, Fujiwara Y, Komohara Y, Yano H, Saito Y, Sugimoto M, Wakita D, Motoshima T, Murakami Y, Yatsuda J, Takahashi N, Suzu S, Asano K, Tamada K and Kamba T. Dysfunction of sinus macrophages in tumor-bearing host induces resistance to immunotherapy. Cancer Sci 2024; 115: 59-69.

[7] Lopez-Yrigoyen M, Cassetta L and Pollard JW. Macrophage targeting in cancer. Ann N Y Acad Sci 2021; 1499: 18-41.

[8] Guan W, Li F, Zhao Z, Zhang Z, Hu J and Zhang Y. Tumor-associated macrophage promotes the survival of cancer cells upon docetaxel chemotherapy via the CSF1/CSF1R-CXCL12/CXCR4 axis in castration-resistant prostate cancer. Genes (Basel) 2021; 12: 773.

[9] Zhou S, Zhu J, Xu J, Gu B, Zhao Q, Luo C, Gao Z, Chin YE and Cheng X. Anti-tumour potential of PD-L1/PD-1 post-translational modifications. Immunology 2022; 167: 471-481.

[10] Lin Y, Luo S, Luo M, Lu X, Li Q, Xie M, Huang Y, Liao X, Zhang Y, Li Y and Liang R. Homologous recombination repair gene mutations in colorectal cancer favors treatment of immune

checkpoint inhibitors. Mol Carcinog 2023; 62: 1271-1283.
[11] Cui Z, Wang Q, Deng M, Meng E, Liu S, Niu B, and Han Q. Long-term response to sintilimab, bevacizumab and chemotherapy in heavily pretreated microsatellite stable colon cancer. Immunotherapy 2023; 15: 127-133.
[12] Qin R, Ren W, Ya G, Wang B, He J, Ren S, Jiang L and Zhao S. Role of chemokines in the crosstalk between tumor and tumor-associated macrophages. Clin Exp Med 2023; 23: 1359-1373.
[13] Qiao H, Lv R, Pang Y, Yao Z, Zhou X, Zhu W and Zhou W. Weighted gene coexpression network analysis identifies TBC1D10C as a new prognostic biomarker for breast cancer. Anal Cell Pathol (Amst) 2022; 2022: 5259187.
[14] Geng S, Fu Y, Fu S and Wu K. A tumor microenvironment-related risk model for predicting the prognosis and tumor immunity of breast cancer patients. Front Immunol 2022; 13: 927565.
[15] Falcomatà C, Bärthel S, Widholz SA, Schneeweis C, Montero JJ, Toska A, Mir J, Kaltenbacher T, Heetmeyer J, Swietlik JJ, Cheng JY, Teodorescu B, Reichert O, Schmitt C, Grabichler K, Coluccio A, Boniolo F, Veltkamp C, Zukowska M, Vargas AA, Paik WH, Jesinghaus M, Steiger K, Maresch R, Öllinger R, Ammon T, Baranov O, Robles MS, Rechenberger J, Kuster B, Meissner F, Reichert M, Flossdorf M, Rad R, Schmidt-Supprian M, Schneider G and Saur D. Selective multi-kinase inhibition sensitizes mesenchymal pancreatic cancer to immune checkpoint blockade by remodeling the tumor microenvironment. Nat Cancer 2022; 3: 318-336.
[16] Wang Y, Cui K, Zhu M and Gu Y. Coexpression module construction by weighted gene coexpression network analysis and identify potential prognostic markers of breast cancer. Cancer Biother Radiopharm 2022; 37: 612-623.
[17] Wu K, Lin K, Li X, Yuan X, Xu P, Ni P and Xu D. Redefining tumor-associated macrophage subpopulations and functions in the tumor microenvironment. Front Immunol 2020; 11: 1731.
[18] Wu J, Li K, Peng W, Li H, Li Q, Wang X, Peng Y, Tang X and Fu X. Autoinducer-2 of fusobacterium nucleatum promotes macrophage M1 polarization via TNFSF9/IL-1β signaling. Int Immunopharmacol 2019; 74: 105724.
[19] He Q, Qu M, Shen T, Xu Y, Luo J, Tan D, Xu C, Barkat MQ, Zeng LH and Wu X. Suppression of VEGFD expression by S-nitrosylation promotes the development of lung adenocarcinoma. J Exp Clin Cancer Res 2022; 41: 239.
[20] Wu W, Jia L, Zhang Y, Zhao J, Dong Y and Qiang Y. Exploration of the prognostic signature reflecting tumor microenvironment of lung adenocarcinoma based on immunologically relevant genes. Bioengineered 2021; 12: 7417-7431.
[21] Zhou Y, Wang S, Zhao J and Fang P. Correlations of complication with coronary arterial lesion with VEGF, PLT, D-dimer and inflammatory factor in child patients with Kawasaki disease. Eur Rev Med Pharmacol Sci 2018; 22: 5121-5126.
[22] Levine KM, Ding K, Chen L and Oesterreich S. FGFR4: a promising therapeutic target for breast cancer and other solid tumors. Pharmacol Ther 2020; 214: 107590.
[23] Ji L, Lin Z, Wan Z, Xia S, Jiang S, Cen D, Cai L, Xu J and Cai X. miR-486-3p mediates hepatocellular carcinoma sorafenib resistance by targeting FGFR4 and EGFR. Cell Death Dis 2020; 11: 250.
[24] Deng Z, Cui L, Li P, Ren N, Zhong Z, Tang Z, Wang L, Gong J, Cheng H, Guan Y, Yi X, Xia X, Zhou R and He Z. Genomic comparison between cerebrospinal fluid and primary tumor revealed the genetic events associated with brain metastasis in lung adenocarcinoma. Cell Death Dis 2021; 12: 935.
[25] Lang L and Teng Y. Fibroblast growth factor receptor 4 targeting in cancer: new insights into mechanisms and therapeutic strategies. Cells 2019; 8: 31.
[26] Hu X, Liu H and Li C. MiRNA-19b-3p downregulates the endothelin B receptor in gastric cancer cells to prevent angiogenesis and proliferation. Acta Biochim Pol 2023; 70: 363-370.
[27] Khan MA, Khan P, Ahmad A, Fatima M and Nasser MW. FOXM1: a small fox that makes more tracks for cancer progression and metastasis. Semin Cancer Biol 2023; 92: 1-15.
[28] Liu S, Zhang J, Zhu J, Jiao D and Liu Z. Prognostic values of EDNRB in triple-negative breast cancer. Oncol Lett 2020; 20: 149.
[29] Zhang Q, Zhang R, Liu M, Wu H and Yang B. An integrated model of CDCA5 and FOXM1 expression combined with a residual disease that predicts prognosis in ovarian cancer patients. Cell Mol Biol (Noisy-le-grand) 2023; 69: 143-149.
[30] Kubli SP, Berger T, Araujo DV, Siu LL and Mak TW. Beyond immune checkpoint blockade: emerging immunological strategies. Nat Rev Drug Discov 2021; 20: 899-919.
[31] Chen ZY, Duan XT, Qiao SM and Zhu XX. Radiotherapy combined with PD-1/PD-L1 inhibitors in NSCLC brain metastases treatment: the mechanisms, advances, opportunities, and challenges. Cancer Med 2023; 12: 995-1006.
[32] Papavassiliou KA, Marinos G and Papavassiliou AG. Targeting YAP/TAZ in combination with PD-

L1 immune checkpoint inhibitors in non-small cell lung cancer (NSCLC). Cells 2023; 12: 871.
[33] Steendam CMJ, Ernst SM, Badrising SK, Paats MS, Aerts JGJV, de Langen AJ and Dingemans AC. Chemotherapy for patients with EGFR-mutated NSCLC after progression on EGFR-TKI's: exploration of efficacy of unselected treatment in a multicenter cohort study. Lung Cancer 2023; 181: 107248.